Published in final edited form as:
Brain Struct Funct. 2014 January ; 219(1): . doi:10.1007/s00429-013-0503-0.

Corpus callosum shape changes in early Alzheimer's disease: an MRI study using the OASIS brain database

Babak A. Ardekani,
The Nathan S. Kline Institute for Psychiatric Research, 140 Old Orangeburg Road, Orangeburg, NY 10962, USA

Department of Psychiatry, New York University School of Medicine, 550 1st Avenue, New York, NY 10016, USA

Center for Advanced Brain Imaging, Nathan Kline Institute, 140 Old Orangeburg Rd, Orangeburg, NY 10962, USA

Alvin H. Bachman,
The Nathan S. Kline Institute for Psychiatric Research, 140 Old Orangeburg Road, Orangeburg, NY 10962, USA

Khadija Figarsky, and
The Nathan S. Kline Institute for Psychiatric Research, 140 Old Orangeburg Road, Orangeburg, NY 10962, USA

John J. Sidtis
The Nathan S. Kline Institute for Psychiatric Research, 140 Old Orangeburg Road, Orangeburg, NY 10962, USA

Department of Psychiatry, New York University School of Medicine, 550 1st Avenue, New York, NY 10016, USA

Babak A. Ardekani: ardekani@nki.rfmh.org

Abstract

The corpus callosum (CC) is the largest fiber bundle connecting the left and right cerebral hemispheres. It has been a region examined extensively for indications of various pathologies, including Alzheimer's disease (AD). Almost all previous studies of the CC in AD have been concerned with its *size*, particularly its mid-sagittal cross-sectional area (CCA). In this study, we show that the CC *shape*, characterized by its *circularity* (CIR), may be affected more profoundly than its size in early AD. MRI scans (n = 196) were obtained from the publicly available Open Access Series of Imaging Studies database. The CC cross-sectional region on the mid-sagittal section of the brain was automatically segmented using a novel algorithm. The CCA and CIR were compared in 98 normal controls (NC) subjects, 70 patients with very mild AD (AD-VM), and 28 patients with mild AD (AD-M). Statistical *analysis of covariance* controlling for age and intracranial capacity showed that both the CIR and the CCA were significantly reduced in the AD-VM group relative to the NC group (CIR: p = 0.004; CCA: p = 0.005). However, only the CIR was significantly different between the AD-M and AD-VM groups (p = 0.006) being smaller in the former. The CCA was not significantly different between the AD-M and AD-VM groups. The results suggest that CC shape may be a more sensitive marker than its size for monitoring the progression of AD. In order to facilitate independent analyses, the CC segmentations and the CCA

Correspondence to: Babak A. Ardekani, ardekani@nki.rfmh.org.

and CIR data used in this study have been made publicly available (http://www.nitrc.org/projects/art).

Keywords

Alzheimer's disease; Brain; Corpus callosum; Shape analysis; Magnetic resonance imaging

Introduction

The corpus callosum (CC) is the largest fiber bundle connecting the two cerebral hemispheres. Atrophy of the CC may lead to functional disability because of reduced interhemispheric integration. It is a region that has been examined intensively for indications of various pathologies, ranging from dyslexia (Hynd et al. 1995), bipolar disorder (Yasar et al. 2006), and Schizophrenia (Downhill et al. 2000) to Alzheimer's disease (AD) (Di Paola et al. 2010b; Frederiksen et al. 2011; Hallam et al. 2008; Hampel et al. 1998; Hensel et al. 2002; Janowsky et al. 1996; Ryberg et al. 2011; Teipel et al. 2002, 2003; Thomann et al. 2006; Wang et al. 2006; Zhu et al. 2012). This is due, in part, to its size, its widespread cortical projections, and its unambiguous signal with contemporary neuroimaging techniques. As the mid-sagittal section of the CC is fairly well defined, it has been the primary focus of examination. Techniques have evolved from post-mortem sectioning to magnetic resonance imaging (MRI) of the living human brain, and from manual tracing of photographs to automatic computer techniques. Recent advances have included diffusion tensor imaging (DTI), T1-weighted high-resolution imaging, and automatic segmentation algorithms. A review of in vivo structural studies of CC in AD and mild cognitive impairment (MCI) using different MRI techniques is given by Di Paola et al. (2010c).

As the field has progressed, it has become apparent that the size and shape of the CC depends on age (Ardekani et al. 2012b), handedness (Witelson 1985; Luders et al. 2010), brain size and sex (Holloway et al. 1993; Smith 2005; Ardekani et al. 2012b), as well as the presence of pathology. Many of the earlier papers dealt with small sample sizes and lower resolution images, and did not account for these confounding variables in their analyses. As a result, some of the previous studies have reported conflicting findings, for example, whether callosal atrophy occurs early in the dementing process (Wang et al. 2006) or is present predominately in the later stages of AD (Di Paola et al. 2010b), whether the size of the CC declines with age in patients with AD or remains unchanged (Janowsky et al. 1996), and whether atrophy primarily occurs in the anterior regions of the CC (Thomann et al. 2006; Zhu et al. 2012), the posterior regions (Frederiksen et al. 2011; Wang et al. 2006), or both (Di Paola et al. 2010a; Teipel et al. 2002; Hallam et al. 2008).

It has been posited that two different mechanisms might contribute to CC atrophy in AD: the death of cells in the gray matter, particularly the large pyramidal cells in cortical layer III, resulting in Wallerian degeneration of axons in the white matter; and direct myelin breakdown of callosal fibers (Di Paola et al. 2010a). To this date, morphological studies of CC in AD have been mainly concerned with size reflecting these degenerative processes. However, in addition to these effects, the CC shape may change because of ventricular dilation reflecting an overall brain atrophic process. The aim of the current study was to examine CC shape in AD using *circularity* as a descriptive parameter. Since circularity captures not only area changes due to CC atrophy but also changes in the CC perimeter due to deformation, we hypothesized that circularity may be a more sensitive indicator of disease progression than cross-sectional area. Using the publically available Open Access Series of Imaging Studies (OASIS) MRI database (Marcus et al. 2007), we compared circularity with cross-sectional area. We made our segmentation results and corresponding measurements

publically available (http://www.nitrc.org/projects/art) to allow independent cross checking of our results and to encourage data sharing which could be of benefit to the neuroimaging community (Poline et al. 2012).

Methods

MRI volumes

We used 196 MRI scans (from the total of 416) available in the OASIS cross-sectional dataset. The MRI scans are three-dimensional (3D) sagittal T1-weighted volumes of matrix size: 256 × 256 × 128 and voxel size: 1 × 1 × 1.25 mm^3. Each volume is the post-registration average of 3 or 4 independently acquired magnetization prepared rapid gradient-echo (MP-RAGE) scans with repetition time (TR): 9.7 ms; echo time (TE): 4.0 ms; inversion time (TI): 20 ms; delay time (TD): 200 ms; and flip angle: 10°; obtained using a 1.5 T Siemens Vision scanner (Erlangen, Germany). More details can be found in Marcus et al. (2007).

Subjects

The 196 subjects included 98 normal controls (NC) aged 60 YEARS or above in the OASIS cross-sectional dataset with a Clinical Dementia Rating (CDR) scale (Morris 1993) of zero; 70 subjects clinically diagnosed with very mild AD (AD-VM) with CDR = 0.5; and 28 subjects with mild AD (AD-M) with CDR = 1. Details of the method for diagnosis and classification of subjects into NC, AD-VM, and AD-M are given in Marcus et al. (2007). Briefly, “the determination of AD or control status was based solely on clinical methods, without reference to psychometric performance, and any potential alternative causes of dementia (known neurological, medical, or psychiatric disorders) had to be absent. The diagnosis of AD was based on clinical information (derived primarily from a collateral source) that the subject had experienced gradual onset and progression of decline in memory and other cognitive and functional domains. Dementia status was established and staged using the CDR scale, a dementia-staging instrument that rates subjects for impairment in each of the six domains: memory, orientation, judgment and problem solving, function in community affairs, home and hobbies, and personal care. Based on the collateral source and subject interview, a global CDR score was derived from individual ratings in each domain. A global CDR of 0 indicates no dementia, and CDRs of 0.5, 1, 2, and 3 represent very mild, mild, moderate, and severe dementia, respectively.”

All subjects were right-handed. Subject demographics are summarized in Table 1. Details of subject recruitment and evaluation methods, inclusion and exclusion criteria, and other characteristics are given by Marcus et al. (2007). Briefly, according to Marcus et al. “the older subjects in the OASIS cross-sectional database with and without dementia were obtained from the longitudinal pool of the Washington University Alzheimer Disease Research Center (ADRC). Subjects with a primary cause of dementia other than AD (e.g., vascular dementia, primary progressive aphasia), active neurological or psychiatric illness (e.g., major depression), serious head injury, history of clinically meaningful stroke, and use of psychoactive drugs were excluded, as were subjects with gross anatomical abnormalities evident in their MRI images (e.g., large lesions, tumors). However, subjects with age-typical brain changes (e.g., mild atrophy, leukoaraiosis) were accepted.”

Corpus callosum segmentation

We used a fully automated method to find the mid-sagittal plane (MSP) of the MRI volumes (Ardekani et al. 1997) to bring the head yaw and roll angles as close as possible to zero. Uncorrected head tilt within the scanner during MRI acquisition has been shown to introduce errors in CC measurements (Rauch and Jinkins 1996). In addition, the anterior

commissure (AP) and posterior commissure (PC) were located on the MSP using a fully automated model-based method (Ardekani and Bachman 2009). Using this information, the original MRI volume was re-sliced to obtain a single image of matrix size: 512 × 512 and pixel size: 0.5 × 0.5 mm^2 representing the true AC-PC aligned MSP (Fig. 1). Using a priori information obtained from manually traced corpora callosa on this type of image, a rectangular CC search region was indentified on the MSP as shown in Fig. 1. Finally, a multi-atlas model-based segmentation method (Aljabar et al. 2009; Cabezas et al. 2011; Ardekani et al. 2012a, b) using the Automatic Registration Toolbox (ART) non-linear registration algorithm (Ardekani et al. 2005; Klein et al. 2009) was used to locate the CC within the search region as shown in Fig. 1. Our serial implementation of the entire segmentation process with 38 atlases takes less than 1 min on a Linux workstation with 2.4 GHz clock speed. ART is a non-linear registration algorithm that searches for a displacement vector at each voxel in the target image, with the speed of the algorithm being approximately proportional to the number of voxels processed. In the current application, the displacement field is only sought for the voxels comprising the search region shown in Fig. 1 which are a small fraction of the total number of voxels in a 3D MRI volume. Therefore, the time required for non-linear registration of an atlas to the target is only a fraction of the time that would normally be required to register a full 3D MRI volume, which explains the relatively fast speed of our CC segmentation method.

Further details of the multi-atlas segmentation method are given in Ardekani et al. (2012a, b). Briefly, all 38 atlases were registered to the test image. However, at each voxel, a subset of m atlases were selected using a local correlation coefficient (LCC) similarity metric and used to classify the voxel as CC or non-CC using the *vote rule* (Rohlfing et al. 2004). The algorithm is adaptive in that the subset of m atlases used varies from voxel to voxel. The optimum number of atlases was found to be $m = 12$ and the LCC window size 7 × 7 mm^2 using a leave-one-out cross-validation procedure within the training set of 38 atlases.

Every CC segmentation was visually inspected and if necessary, small corrections to the detected CC were made manually using the ITK-SNAP software (Yushkevich et al. 2006) by an operator (KF) who was blind to the subject status. This was necessary in approximately 20 % of the cases. The final segmentation was represented as a binary image where pixels were assigned a value of 1 if they belonged to the CC and a value of 0 otherwise. Morphological operations were performed to ensure that the CC in the binary image is represented as a *4-connected component* with an *Euler number* of one (Jain et al. 1995; cf. Appendix). We have made all 196 automatically detected and AC-PC aligned MSP's (gray level images) and their corresponding segmentations (binary images) publicly available at http://www.nitrc.org/projects/art as supplementary material.

Corpus callosum measurements

We measured the total CC cross-sectional area (CCA) and circularity (CIR) for all 196 subjects in our study. The CCA was measured as the number of pixels comprising the CC in the binary image multiplied by the pixel size of 0.25 mm^2. The CC perimeter was calculated as the length of the 8-path (Jain et al. 1995; cf. Appendix) that constitutes the *border* of the CC. Border pixels were those that were a part of the CC and were 4-neighbors to a non-CC pixel. A border-following algorithm (Jain et al. 1995; cf. Appendix) was used to extract a sequence of pixels that represented the CC border. Two consecutive pixels on the border sequence contributed 0.5 mm to the perimeter if they were 4-neighbors (i.e., shared a side) and $0.5 \times 2^{1/2}$ mm otherwise (i.e., if they only shared a corner). Definition of technical terms such as 4-neighborhood, 4-connectedness, Euler number, etc., and the border following algorithm are given in the Appendix.

For a given region in 2D with area A and perimeter P, circularity is defined as: $4\pi A/P^2$. The value of circularity ranges from 0 for a line (a degenerate case) to 1 for a circle. This is a measure of shape rather than size. For example, two similar triangles would have the exact same circularity regardless of their area. The CCA and CIR measured from all subjects are provided as supplementary material (http://www.nitrc.org/projects/art).

Statistical analysis

Two-way factorial analysis of covariance (ANCOVA) was performed using the SPSS 15.0 for Windows software with sex (F or M) and diagnostic group (NC, AD-VM, or AD-M) as fixed between-subject factors, age, and *intracranial* capacity as covariates, and CCA or CIR as the dependent variable. Post hoc pair-wise tests were planned to ascertain any group differences. Statistical significance was tested at the level of $\alpha = 0.05$ (two-tailed). To control for *intracranial capacity*, we used the variable $eTIV^{2/3}$ where eTIV is the estimate of the total intracranial volume obtained using the method of Buckner et al. (2004) and provided in the OASIS database. The reason for using the allometric exponent 2/3 is discussed in detail by Smith (2005). Briefly, it is due to the fact that in a perfectly isometrically scaling organism all surface area-based properties would change proportionally with volume to the power 2/3. Jäncke et al. (1997) also present evidence that supports the use of 2/3 allometric exponent in relating CC size to a measure of brain size.

Results

The unadjusted means (±SE) for the CCA and CIR are given in Table 1. The ANCOVA results are presented below for each dependent variable separately.

Corpus callosum cross-sectional area

Before conducting the ANCOVA, we tested the assumption of homogeneity of the regression slopes. The test evaluates the interaction between the covariates (age and $eTIV^{2/3}$) and the between-subject factors (sex and diagnosis) in predicting the dependent variable (CCA). There were no significant (sex × age), (sex × $eTIV^{2/3}$), (diagnosis × age), or (diagnosis × $eTIV^{2/3}$) interactions. This means that the slopes of the linear relationships between CCA and $eTIV^{2/3}$, and CCA and age can be assumed the same for the three diagnostic groups (NC, AD-VM, and AD-M) and the two gender groups (male and female). In addition, Levene's test of equality of error variances within each of the 6 (sex × diagnosis) groups showed that the underlying ANCOVA assumption of homogeneity of variance has been met [$F(5, 190) = 0.9$, $p = 0.469$]. ANCOVA showed that: (1) there was a significant age effect on CCA [$F(1,188) = 50.9$; $p < 10^{-10}$; partial $\eta^2 = 0.213$]. As shown in Fig. 2, CCA decreases with age. (2) The intracranial capacity variable $eTIV^{2/3}$ had a significant effect on CCA [$F(1,188) = 39.1$; $p < 10^{-8}$; partial $\eta^2 = 0.172$]. As shown in Fig. 3, CCA increases with intracranial capacity. (3) There was no significant interaction between sex and diagnosis factors [$F(2, 188) = 1.1$; $p = 0.320$]. (4) The main effect of sex was not statistically significant but showed a trend toward females having larger CCA [$F(1, 188) = 3.5$; $p = 0.063$] (adjusted for age and intracranial capacity). (5) The main effect of diagnosis was statistically significant [$F(2,188) = 6.8$; $p = 0.001$; partial $\eta^2 = 0.067$].

The marginal CCA means (adjusted for age and intracranial capacity) of the three diagnostic groups are shown in Fig. 4 and are given in Table 1. CCA decreases with dementia severity. Post hoc pairwise comparisons showed a significance difference between the marginal means of the NC and AD-VM groups ($p = 0.005$), and the NC and AD-M groups ($p = 0.002$). However, there was no statistically significant difference between the AD-VM and AD-M groups ($p = 0.266$).

Corpus callosum circularity

Before conducting the ANCOVA, we tested the assumption of homogeneity of the regression slopes. There were no significant (sex × age), (sex × $eTIV^{2/3}$), (diagnosis × age), or (diagnosis × $eTIV^{2/3}$) interactions. Therefore, the slopes of the linear relationships between CIR and $eTIV^{2/3}$ and between CIR and age were assumed the same for the three diagnostic groups and the two gender groups. Levene's test of equality of error variance showed that the underlying ANCOVA assumption of homogeneity of variance has been met [$F(5, 190) = 1.1$, $p = 0.337$]. ANCOVA showed that: (1) there was a significant age effect on CIR [$F(1,188) = 52.7$; $p < 10^{-10}$; partial $\eta^2 = 0.219$]. As shown in Fig. 5, circularity decreases with age. (2) The intracranial capacity variable $eTIV^{2/3}$ had a significant effect on CIR [$F(1,188) = 38.9$; $p < 10^{-8}$; partial $\eta^2 = 0.171$]. As shown in Fig. 6, circularity decreases with intracranial capacity. (3) There was no significant interaction between sex and diagnosis factors [$F(2, 188) = 2.6$; $p = 0.074$]. (4) The main effect of sex was statistically significant [$F(1, 188) = 6.0$; $p = 0.015$; partial $\eta^2 = 0.031$]. (5) The main effect of diagnosis was also statistically significant [$F(2,188) = 13.1$; $p < 10^{-5}$; partial $\eta^2 = 0.122$].

The corrected CIR means (adjusted for age and intracranial capacity) of the male and female groups are shown in Fig. 7. In this age group, the female CC is less circular than the male counterpart of the same age and intracranial capacity.

The corrected CIR means of the three diagnostic groups are shown in Fig. 8 and are given in Table 1. CIR decreases with dementia severity. Post hoc pairwise comparisons showed a significance difference between the corrected means of the NC and AD-VM groups ($p = 0.004$); NC and AD-M groups ($p < 10^{-5}$); and AD-VM and AD-M groups ($p = 0.006$).

Discussion

To best of our knowledge, this is the first study of the changes in CC circularity, which is a measure of shape rather than size, in AD. We found that in normal subjects and in very mild to mild AD patients aged 60 years or above, the CC shape becomes less circular with age. In addition, we found that the CC shape in larger brains (as indicated by $eTIV^{2/3}$) tends to be less circular. Furthermore, our analysis suggests that the shape of the CC may be sexually dimorphic, being slightly less circular in females. Sexual dimorphism of the CC size has been studied extensively (Holloway et al. 1993; Smith 2005; Ardekani et al. 2012b), however, this is one of the few studies to suggest gender-based shape differences. As far as we are aware, the only other study that investigated sexual dimorphism in the circularity of the whole CC was a postmortem study of 33 adult human brains by Going and Dixson (1990) who did not find a significant gender effect ($p = 0.17$). However, they used an independent samples *t* test without correcting for brain size and age, which we have shown to affect circularity. In addition, post-mortem brains undergo deformations during fixation and dissection which may have adversely affected the study. It must be emphasized that the sex difference in circularity reported here is for older adults (age ≥ 60 years). We have not found evidence that this result holds for younger adults.

Circularity of a shape in 2D is given by $4\pi A/P^2$. Thus, a decrease in circularity could be explained by a decrease in area (A), an increase in perimeter (P), or from a combination of both factors.

Thus, a reduction in CCA either due to the death of cells in the gray matter, particularly the large pyramidal cells in cortical layer III, resulting in Wallerian degeneration of axons in the white matter, or due to direct myelin breakdown of callosal fibers (Di Paola et al. 2010a) would contribute to a reduction in CIR. Reduction in CIR could also result from a pure deformation of the CC while the area is conserved. This could be a result of the mechanical

deformation of the CC because of age and disease related enlargements of the lateral ventricles reflecting an overall atrophic process in the brain. For example consider a rectangle of width W and length L ($L > W$). The area and perimeter of this rectangle are: $W \times L$, and ($2W + 2L$), respectively. Now suppose that we stretch the rectangle to half its width and twice its length. The area of the new rectangle would be the same: ($W/2$) × (2L) = $W \times L$. However, its perimeter would now be ($W + 4$L) which is greater than the perimeter of the original rectangle ($2W + 2L$) since $L > W$. Therefore, the overall effect would be a decrease in CIR. In addition, a non-uniform decrease in the CCA could increase the perimeter as it becomes more irregular, thus decreasing the CIR.

Our results also indicated that the mean CCA, while smaller in the AD-M group relative to the AD-VM group, was not statistically significantly different between the two groups ($p = 0.266$). On the other hand, the mean CIR was significantly smaller in the AD-M group than in the AD-VM group ($p < 0.006$). However, failure to detect a statistically significant difference in CCA between AD-M and AD-VM groups does not imply that no true difference exists. It may merely mean that based on sample size and measurement errors the statistical test used was insufficiently powered to detect a true difference. The fact that under the same conditions a significant difference in CIR was detected between these groups, therefore, suggests that CIR may be a more sensitive marker than CCA for monitoring AD progression.

Hensel et al. (2002) also studied the CCA in a group of 33 normal controls, 27 patients with CDR = 0.5 (their “questionable dementia” group), and 23 patients with CDR = 1 (AD-M). As in our study, they found that the callosal size in CDR = 0.5 group was intermediate between normal controls and CDR = 1. However, statistically significant differences were only found between the normal controls and CDR = 1 groups. As the authors noted, absence of a significant difference between patients with questionable dementia (CDR = 0.5) and any other group may be due to a lack of statistical power in their relatively small sample.

The fact that we did not find a statistically significant difference in CCA between AD-M and AD-VM groups is in direct contradiction of a recently published study (Zhu et al. 2012) that used the exact same data (196 subjects from the OASIS cross-sectional dataset). Zhu et al. reported a statistically significant ($p < 0.05$) difference in CCA between the AD-M and AD-VM groups. There are some differences in the statistical analysis methods used in this paper and the Zhu et al. study, in that the latter did not use age as a covariate or sex as a factor in their ANCOVA—both variables are known to affect CCA. Not accounting for variables that introduce systematic variance in the data is more likely to underpower the statistical test, hence introducing Type II errors, than creating spurious findings. Therefore, differences in statistical methodology are unlikely to explain the discrepancy between the results of the two studies. Comparing the SE reported in this study (Table 1) with those reported in Table 2 of Zhu et al. (note that the caption in Table 2 of Zhu et al. states that standard deviations are given where as in fact the reported values are standard errors—confirmed by Zhu et al. through private communication) it can be seen that our standard errors are smaller than those of Zhu et al. Therefore, the discrepancy cannot be attributed to increased uncertainty in our measurements that could result in Type II errors. Comparing the mean values reported in this study (Table 1) with those reported in Table 2 of Zhu et al., it could be seen that the source of discrepancy is that Zhu et al. report a considerably smaller value for the mean CCA in the AD-M group than that observed in this study. At this time, the reason for this difference is not clear. Fortunately, the OASIS database explicitly authorizes redistribution of data derived from their database. Therefore, we have made our CC segmentations and area measurements available publicly as supplementary material to facilitate comparisons and independent re-analyses of the data. It is hoped that the availability of this completely transparent and easily accessible dataset would help in resolving this discrepancy as well as

other inconsistencies between results reported in the literature concerning CC size and shape in AD.

Di Paola et al. (2010b) using voxel-based morphometry (VBM) found significant CC atrophy in *severe* AD patients as compared to normal controls, but did not detect significant differences between healthy controls, mild AD, or amnestic MCI patients. Thus, they concluded that callosal atrophy is present predominately in the latest stage of AD. In contrast, the results of this paper show that both CC size and shape are significantly affected in patients with very mild AD. An explanation for this discrepancy may be that VBM, which is a generic method, is less sensitive in detecting discrete structural CC changes than the methods used in our study that are specifically designed for accurate CC measurements. Thomann et al. (2006) compared VBM and manual tracing methods for studying CC atrophy in MCI and AD and concluded that VBM is less sensitive than manual tracing in detecting subtle CC differences.

Our analysis showed that both CCA and CIR decrease with increasing age. As far as we are aware, changes in the CC shape, as measured by CIR, with age have not been reported previously. Our finding of CCA changes with age are consistent with the results of Janowsky et al. (1996) who found that CCA showed a significant decline with age in healthy elderly subjects and in a group of “incipient dementia” subjects who were cognitively normal at the time of their MRI study but subsequently developed MCI as indicated by a CDR of 0.5 or greater on two successive 6-month follow-up visits. However, Janowsky et al. did not find an age-related decline in CCA in a group of AD patients ($\rho = -0.15$; $p < 0.354$), while we found a significant negative correlation between age and CCA in both NC and AD patients. A separate analysis performed only on our group of 98 AD patients (70 AD-VM plus 28 AD-M) confirmed a significant age-related decline ($\rho = -0.349$; $p < 0.001$). More than half of the 39 AD patients studied by Janowsky et al. had CDR ≤ 1 but their cohort also included patients with more than mild AD (CDR > 1) who at the time of imaging already had significant atrophy. This could be one reason to explain why as a whole their AD group did not show significant correlation with age. Another possible reason is that Janowsky et al. used multi-slice 2D sagittal MRI acquisitions with 5 mm slice thickness and did not tilt correct the images, rather, a mid-sagittal slice was selected by inspection for tracing, whereas we used an automated technique (Ardekani et al. 1997) for detecting the MSP on 3D high-resolution MP-RAGE MRI scans, and measured the CCA on the MSP after re-slicing the MRI volume by tri-linear interpolation to zero the yaw and roll angles. The importance of applying a consistent and repeatable method for defining the MSP in all subjects has been emphasized by Rauch and Jinkins (1996) and Mitchell et al. (2003). Regardless, our data which we have made publicly available and is based on a large number of publicly available MRI scans clearly shows that atrophic process of CC in very mild and mild AD (CDR ≤ 1) is not complete, but ongoing with age and disease progression.

Our analysis also showed that intracranial capacity had a significant explanatory contribution to both CCA and CIR models. To the best of our knowledge, our finding that CIR decreases with intracranial capacity has not been previously reported. While there is fairly broad consensus that CCA increases with brain size, this has not been found to be the case in some studies (Teipel et al. 2002).

We did not attempt to localize atrophy within the CC. To this date, the majority of methods for subdividing the CC have been purely geometrically based (e.g., splenium as the posterior fifth of CC) (Witelson 1985; Weis et al. 1991; Hampel et al. 1998). However, it has been shown that significant variability can be introduced into the measurements with different methods of subdivision (Constant and Ruther 1996). We believe that using the standard methods of subdivision would make analyses excessively prone to Type I and Type II errors.

A more promising and rigorous method for determining exactly which fiber bundles within the CC are affected by AD will be to use fiber tracking based on DTI to segment the CC into anatomically more meaningful subsections (Abe et al. 2004; Hofer and Frahm 2006). DTI data, however, is not available in OASIS and this remains a topic for future investigation. To this end, our group is also considering the analysis of continuous thickness curves derived along the CC length using the methods of functional data analysis (Ramsay and Silverman 2005).

Conclusions

This study examined 196 high-resolution T1-weighted images from the OASIS shared neuroimaging data resource. The CC was segmented on all images and its area, perimeter, and circularity were measured. These data were analyzed in this paper and made publicly available to the research community for re-examination and analysis. It is hoped that this approach would help resolve some of the discrepancies that exist in the literature concerning the morphology of CC in AD.

This paper also for the first time examined the circularity of the CC in AD alongside its size. Our analysis indicates that: (a) both CIR and CCA decrease with age; (b) CIR decreases and CCA increases with intracranial capacity; (c) the CIR is reduced and CCA is larger in females; and (d) CIR is more sensitive than CCA in distinguishing between the three groups of NC, AD-VM, and AD-M, thus, it appears to be a better measure for tracking AD progression.

Acknowledgments

We thank our colleagues responsible for the OASIS project for making the MRI data available. Data analysis and manuscript preparation were supported by R01 DC007658. The OASIS project was supported by the following NIH grants: P50 AG05681, P01 AG03991, R01 AG021910, P50 MH071616, U24 RR021382, and R01 MH56584.

Appendix

This section provides brief definitions of some of the technical image processing terms used in this paper and the border following algorithm. These are taken from Jain et al. (1995) where more details can be found.

Definition 1 Consider pixels to be square areas with 4 sides and 4 corners. Two pixels (squares) are *4-neighbors* if they share a common side. Two pixels are *8-neighbors* if they share a common side or a common corner.

Definition 2 An *8-path* from pixel 1 to pixel n is sequence of pixels with indices $p_1, p_2,\ldots, p_n$ such that pixels p_k and p_{k+1} ($1 \leq k < n$) are 8-neighbors. Similarly if the pixels are 4-neighbors, the path is referred to as a *4-path*.

Definition 3 A set of pixels in which each pixel is connected to all other pixels by a 4-path is called a *4-connected component*. Similarly, if each pixel is connected to all other pixels by an 8-path, the set of pixels is referred to as an *8-connected component*.

Definition 4 The *Euler number* is defined as the number of components in an object minus the number of holes. Therefore, the Euler number of a 4- or 8-connected component equals 1 if it does not have any holes.

Definition 5 The *border* of a connected component S is all pixels of S that have at least one 4-neighbor that is not in S.

Border-following algorithm: (a) Find a starting border pixel s of connected component S by scanning the image systematically from left to right and from top to bottom. (b) Let the current pixel in the border be denoted by c. Set $c = s$ and let the 4-neighbor to the west of s be b. Note that b will not be in S. (c) Let the eight 8-neighbors of c starting with b in clockwise order be $n_1, n_2, \ldots, n_8$. Find n_i, for the first i that is in S. (d) Set $c = n_i$ and $b = n_{i-1}$. (e) Repeat steps (c) and (d) until $c = s$.

References

Abe O, Masutani Y, Aoki S, Yamasue H, Yamada H, Kasai K, Mori H, Hayashi N, Masumoto T, Ohtomo K. Topography of the human corpus callosum using diffusion tensor tractography. J Comput Assist Tomogr. 2004; 28:533–539. [PubMed: 15232387]

Aljabar P, Heckemann RA, Hammers A, Hajnal JV, Rueckert D. Multi-atlas based segmentation of brain images: atlas selection and its effect on accuracy. Neuroimage. 2009; 46:726–738. [PubMed: 19245840]

Ardekani BA, Bachman AH. Model-based automatic detection of the anterior and posterior commissures on MRI scans. Neuroimage. 2009; 46:677–682. [PubMed: 19264138]

Ardekani BA, Kershaw J, Braun M, Kanno I. Automatic detection of the mid-sagittal plane in 3-D brain images. IEEE Trans Med Imaging. 1997; 16:947–952. [PubMed: 9533596]

Ardekani BA, Guckemus S, Bachman A, Hoptman MJ, Wojtaszek M, Nierenberg J. Quantitative comparison of algorithms for inter-subject registration of 3D volumetric brain MRI scans. J Neurosci Methods. 2005; 142:67–76. [PubMed: 15652618]

Ardekani BA, Toshikazu I, Bachman A, Szeszko PR. Multi-atlas corpus callosum segmentation with adaptive atlas selection. Proc Int Soc Magn Reson Med Melbourne, Australia. 2012a Abstract #2564.

Ardekani BA, Figarsky K, Sidtis JJ. Sexual dimorphism in the human corpus callosum: an MRI study using the OASIS brain database. Cereb Cortex. 2012b (in press).

Buckner RL, Head D, Parker J, Fotenos AF, Marcus D, Morris JC, Snyder AZ. A unified approach for morphometric and functional data analysis in young, old, and demented adults using automated atlas-based head size normalization: reliability and validation against manual measurement of total intracranial volume. Neuroimage. 2004; 23:724–738. [PubMed: 15488422]

Cabezas M, Oliver A, Lladó X, Freixenet J, Cuadra MB. A review of atlas-based segmentation for magnetic resonance brain images. Comput Methods Programs Biomed. 2011; 104:e158–e177. [PubMed: 21871688]

Constant D, Ruther H. Sexual dimorphism in the human corpus callosum? A comparison of methodologies. Brain Res. 1996; 727:99–106. [PubMed: 8842387]

Di Paola M, Di Iulio F, Cherubini A, Blundo C, Casini AR, Sancesario G, Passafiume D, Caltagirone C, Spalletta G. When, where, and how the corpus callosum changes in MCI and AD: a multimodal MRI study. Neurology. 2010; 74:1136–1142. [PubMed: 20368633]

Di Paola M, Luders E, Di Iulio F, Cherubini A, Passafiume D, Thompson PM, Caltagirone C, Toga AW, Spalletta G. Callosal atrophy in mild cognitive impairment and Alzheimer's disease: different effects in different stages. Neuroimage. 2010; 49:141–149. [PubMed: 19643188]

Di Paola M, Spalletta G, Caltagirone C. In vivo structural neuroanatomy of corpus callosum in Alzheimer's disease and mild cognitive impairment using different MRI techniques: a review. J Alzheimers Dis. 2010; 20:67–95. [PubMed: 20164572]

Downhill JE Jr, Buchsbaum MS, Wei T, Spiegel-Cohen J, Hazlett EA, Haznedar MM, Silverman J, Siever LJ. Shape and size of the corpus callosum in schizophrenia and schizotypal personality disorder. Schizophr Res. 2000; 42:193–208. [PubMed: 10785578]

Frederiksen KS, Garde E, Skimminge A, Ryberg C, Rostrup E, Baaré WF, Siebner HR, Hejl AM, Leffers AM, Waldemar G. Corpus callosum atrophy in patients with mild Alzheimer's disease. Neurodegener Dis. 2011; 8:476–482. [PubMed: 21659724]

Going JJ, Dixson A. Morphometry of the adult human corpus callosum: lack of sexual dimorphism. J Anat. 1990; 171:163–167. [PubMed: 2081703]

Hallam BJ, Brown WS, Ross C, Buckwalter JG, Bigler ED, Tschanz JT, Norton MC, Welsh-Bohmer KA, Breitner JC. Regional atrophy of the corpus callosum in dementia. J Int Neuropsychol Soc. 2008; 14:414–423. [PubMed: 18419840]

Hampel H, Teipel SJ, Alexander GE, Horwitz B, Teichberg D, Schapiro MB, Rapoport SI. Corpus callosum atrophy is a possible indicator of region- and cell type-specific neuronal degeneration in Alzheimer disease: a magnetic resonance imaging analysis. Arch Neurol. 1998; 55:193–198. [PubMed: 9482361]

Hensel A, Wolf H, Kruggel F, Riedel-Heller SG, Nikolaus C, Arendt T, Gertz HJ. Morphometry of the corpus callosum in patients with questionable and mild dementia. J Neurol Neurosurg Psychiatry. 2002; 73:59–61. [PubMed: 12082047]

Hofer S, Frahm J. Topography of the human corpus callosum revisited-comprehensive fiber tractography using diffusion tensor magnetic resonance imaging. Neuroimage. 2006; 32:989–994. [PubMed: 16854598]

Holloway RL, Anderson PJ, Defendini R, Harper C. Sexual dimorphism of the human corpus callosum from three independent samples: relative size of the corpus callosum. Am J Phys Anthropol. 1993; 92:481–498. [PubMed: 8296877]

Hynd GW, Hall J, Novey ES, Eliopulos D, Black K, Gonzalez JJ, Edmonds JE, Riccio C, Cohen M. Dyslexia and corpus callosum morphology. Arch Neurol. 1995; 52:32–38. [PubMed: 7826273]

Jain, R.; Kasturi, R.; Schunck, BG. Machine vision. New York: McGraw-Hill; 1995.

Jäncke L, Staiger JF, Schlaug G, Huang Y, Steinmetz H. The relationship between corpus callosum size and forebrain volume. Cereb Cortex. 1997; 7:48–56. [PubMed: 9023431]

Janowsky JS, Kaye JA, Carper RA. Atrophy of the corpus callosum in Alzheimer's disease versus healthy aging. J Am Geriatr Soc. 1996; 44:798–803. [PubMed: 8675927]

Klein A, Andersson J, Ardekani BA, Ashburner J, Avants B, Chiang MC, Christensen GE, Collins DL, Gee J, Hellier P, Song JH, Jenkinson M, Lepage C, Rueckert D, Thompson P, Vercauteren T, Woods RP, Mann JJ, Parsey RV. Evaluation of 14 nonlinear deformation algorithms applied to human brain MRI registration. Neuroimage. 2009; 46:786–802. [PubMed: 19195496]

Luders E, Cherbuin N, Thompson PM, Gutman B, Anstey KJ, Sachdev P, Toga AW. When more is less: associations between corpus callosum size and handedness lateralization. Neuroimage. 2010; 52:43–49. [PubMed: 20394828]

Marcus DS, Wang TH, Parker J, Csernansky JG, Morris JC, Buckner RL. Open Access Series of Imaging Studies (OASIS): cross-sectional MRI data in young, middle aged, nondemented, and demented older adults. J Cogn Neurosci. 2007; 19:1498–1507. [PubMed: 17714011]

Mitchell TN, Free SL, Merschhemke M, Lemieux L, Sisodiya SM, Shorvon SD. Reliable callosal measurement: population normative data confirm sex-related differences. AJNR Am J Neuroradiol. 2003; 24:410–418. [PubMed: 12637291]

Morris JC. The Clinical Dementia Rating (CDR): current version and scoring rules. Neurology. 1993; 43:2412–2414. [PubMed: 8232972]

Poline JB, Breeze JL, Ghosh S, Gorgolewski K, Halchenko YO, Hanke M, Haselgrove C, Helmer KG, Keator DB, Marcus DS, Poldrack RA, Schwartz Y, Ashburner J, Kennedy DN. Data sharing in neuroimaging research. Front Neuroinform. 2012; 6:1–13. [PubMed: 22319490]

Ramsay, JO.; Silverman, BW. Functional data analysis. 2nd edn.. New York: Springer; 2005.

Rauch RA, Jinkins JR. Variability of corpus callosal area measurements from midsagittal MR images: effect of subject placement within the scanner. Am J Neuroradial. 1996; 17:27–28.

Rohlfing T, Brandt R, Menzel R, Maurer CR Jr. Evaluation of atlas selection strategies for atlas-based image segmentation with application to confocal microscopy images of bee brains. Neuroimage. 2004; 21:1428–1442. [PubMed: 15050568]

Ryberg C, Rostrup E, Paulson OB, Barkhof F, Scheltens P, van Straaten EC, van der Flier WM, Fazekas F, Schmidt R, Ferro JM, Baezner H, Erkinjuntti T, Jokinen H, Wahlund LO, Poggesi A, Pantoni L, Inzitari D, Waldemar G. LADIS study group. Corpus callosum atrophy as a predictor of age-related cognitive and motor impairment: a 3-year follow-up of the LADIS study cohort. J Neurol Sci. 2011; 307:100–105. [PubMed: 21621224]

Smith RJ. Relative size versus controlling for size: interpretation of ratios in research on sexual dimorphism in the human corpus callosum. Curr Anthropol. 2005; 46:249–273.

Teipel SJ, Bayer W, Alexander GE, Zebuhr Y, Teichberg D, Kulic L, Schapiro MB, Möller HJ, Rapoport SI, Hampel H. Progression of corpus callosum atrophy in Alzheimer disease. Arch Neurol. 2002; 59:243–248. [PubMed: 11843695]

Teipel SJ, Bayer W, Alexander GE, Bokde AL, Zebuhr Y, Teichberg D, Müller-Spahn F, Schapiro MB, Möller HJ, Rapoport SI, Hampel H. Regional pattern of hippocampus and corpus callosum atrophy in Alzheimer's disease in relation to dementia severity: evidence for early neocortical degeneration. Neurobiol Aging. 2003; 24:85–94. [PubMed: 12493554]

Thomann PA, Wustenberg T, Pantel J, Essig M, Schroder J. Structural changes of the corpus callosum in mild cognitive impairment and Alzheimer'sdisease. Dement Geriatr Cogn Disord. 2006; 21:215–220. [PubMed: 16415572]

Wang PJ, Saykin AJ, Flashman LA, Wishart HA, Rabin LA, Santulli RB, McHugh TL, MacDonald JW, Mamourian AC. Regionally specific atrophy of the corpus callosum in AD, MCI and cognitive complaints. Neurobiol Aging. 2006; 27:1613–1617. [PubMed: 16271806]

Weis S, Jellinger K, Wenger E. Morphology of the corpus callosum in normal aging and Alzheimer's disease. J Neural Transm Suppl. 1991; 33:35–38. [PubMed: 1753249]

Witelson SF. The brain connection: the callosum is larger in left-handers. Science. 1985; 229:665–668. [PubMed: 4023705]

Yasar AS, Monkul ES, Sassi RB, Axelson D, Brambilla P, Nicoletti MA, Hatch JP, Keshavan M, Ryan N, Birmaher B, Soares JC. MRI study of corpus callosum in children and adolescents with bipolar disorder. Psychiatry Res. 2006; 146:83–85. [PubMed: 16337778]

Yushkevich PA, Piven J, Hazlett HC, Smith RG, Ho S, Gee JC, Gerig G. User-guided 3D active contour segmentation of anatomical structures: significantly improved efficiency and reliability. Neuroimage. 2006; 31:1116–1128. [PubMed: 16545965]

Zhu M, Gao W, Wang X, Shi C, Lin Z. Progression of corpus callosum atrophy in early stage of Alzheimer's disease: MRI based study. Acad Radiol. 2012; 19:512–517. [PubMed: 22342652]

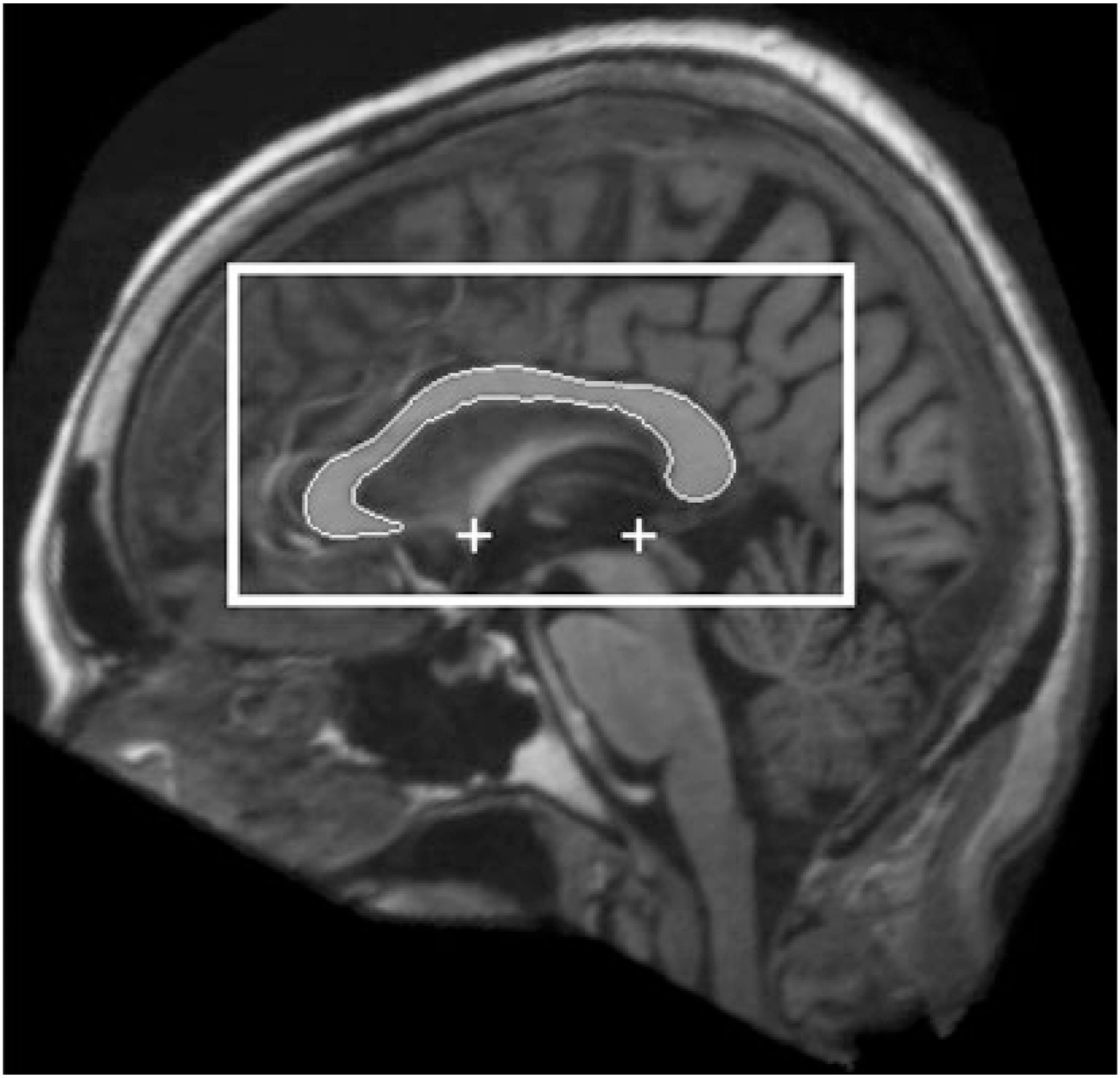

Fig. 1.

The automatically detected mid-sagittal plane (MSP) using the algorithm of Ardekani et al. (1997) is shown in the background. The automatically detected anterior commissure (AC) and posterior commissure (PC) using the algorithm of Ardekani and Bachman (2009) are shown by the *plus signs*. The MSP is aligned so that the AC-PC line is horizontal with respect to the image coordinates. The *rectangular box* shows the search region for the corpus callosum (CC) obtained a priori using 38 manually delineated corpora callosa on AC-PC aligned MSP images as training data. The outline shows the detected CC using the algorithm described in this paper and in more detail in Ardekani et al. (2012a, b)

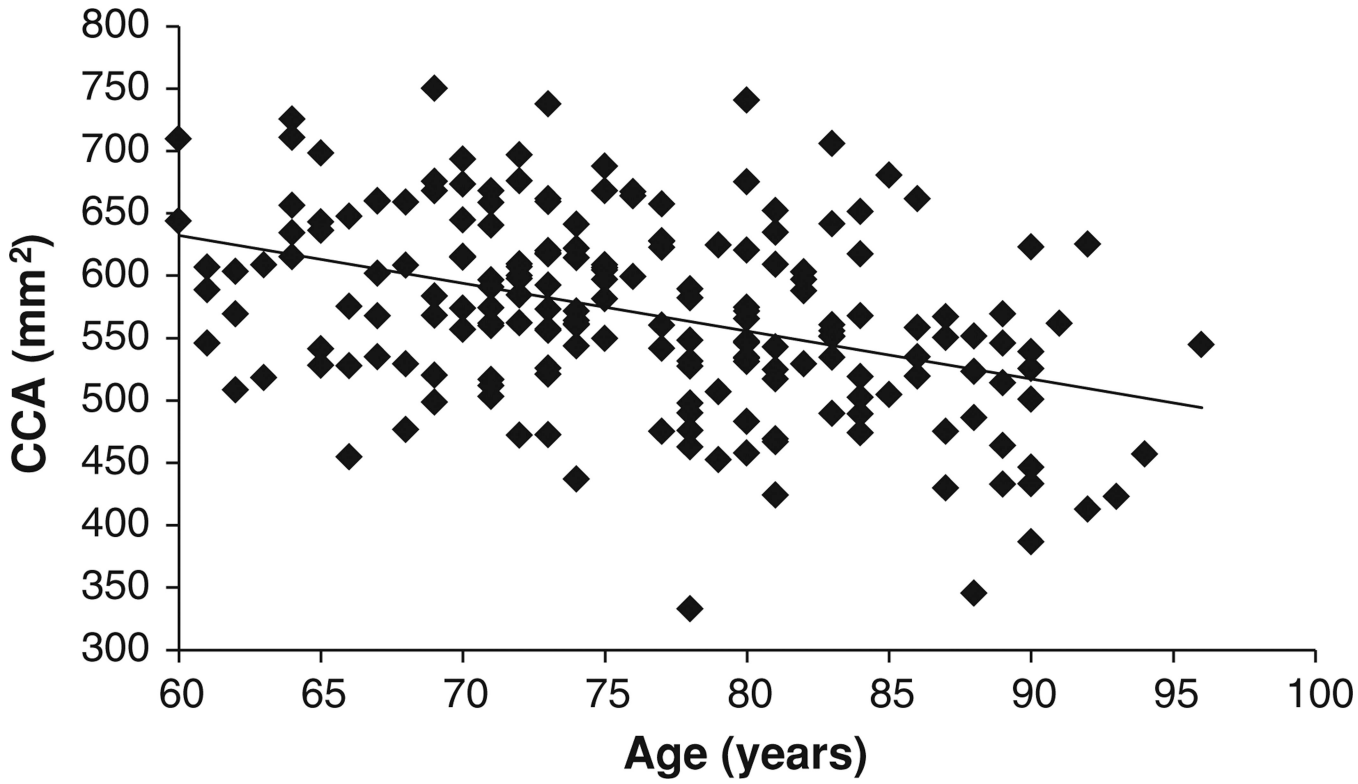

Fig. 2.
Correlation between CCA and age ($\rho = -0.408$; $p < 10^{-8}$)

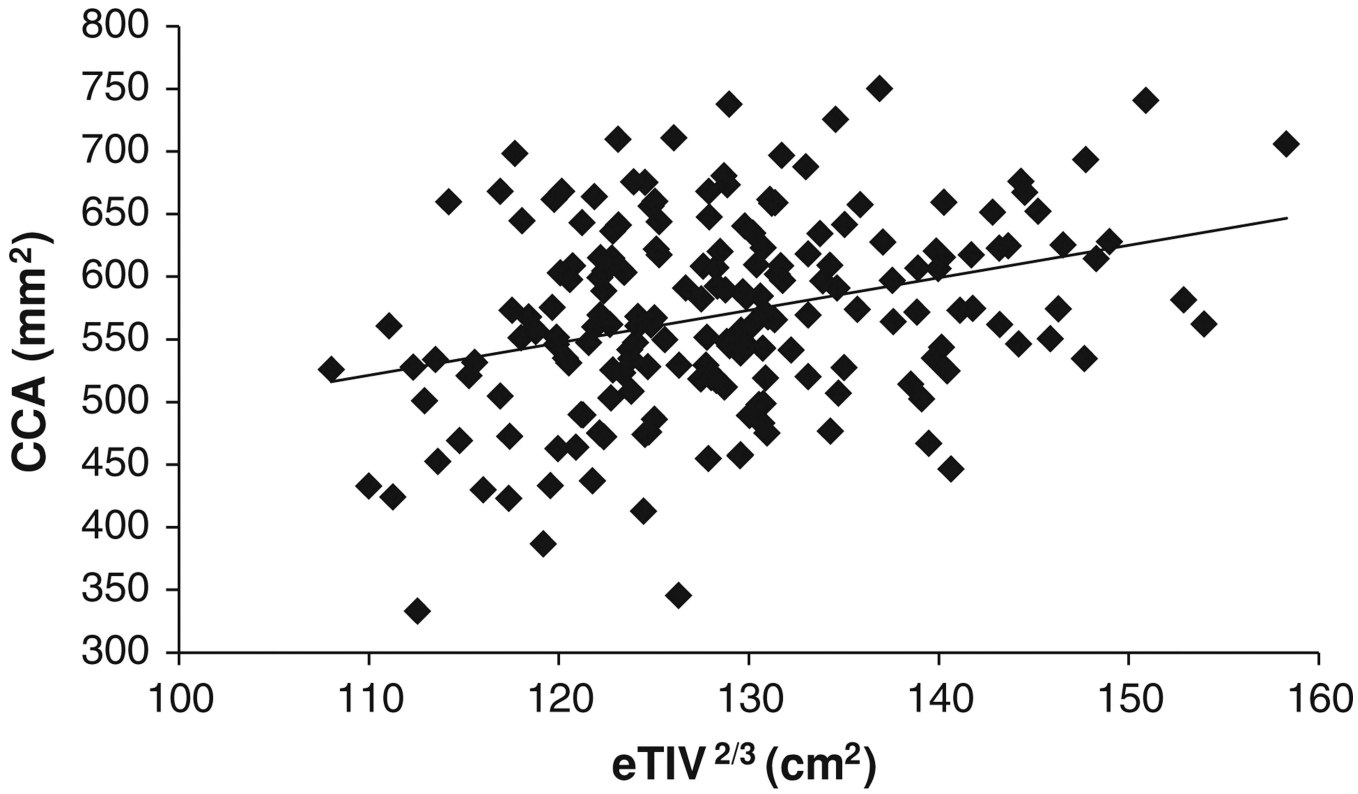

Fig. 3.
Correlation between CCA and intracranial capacity variable $eTIV^{2/3}$ ($\rho = 0.321$; $p < 10^{-5}$)

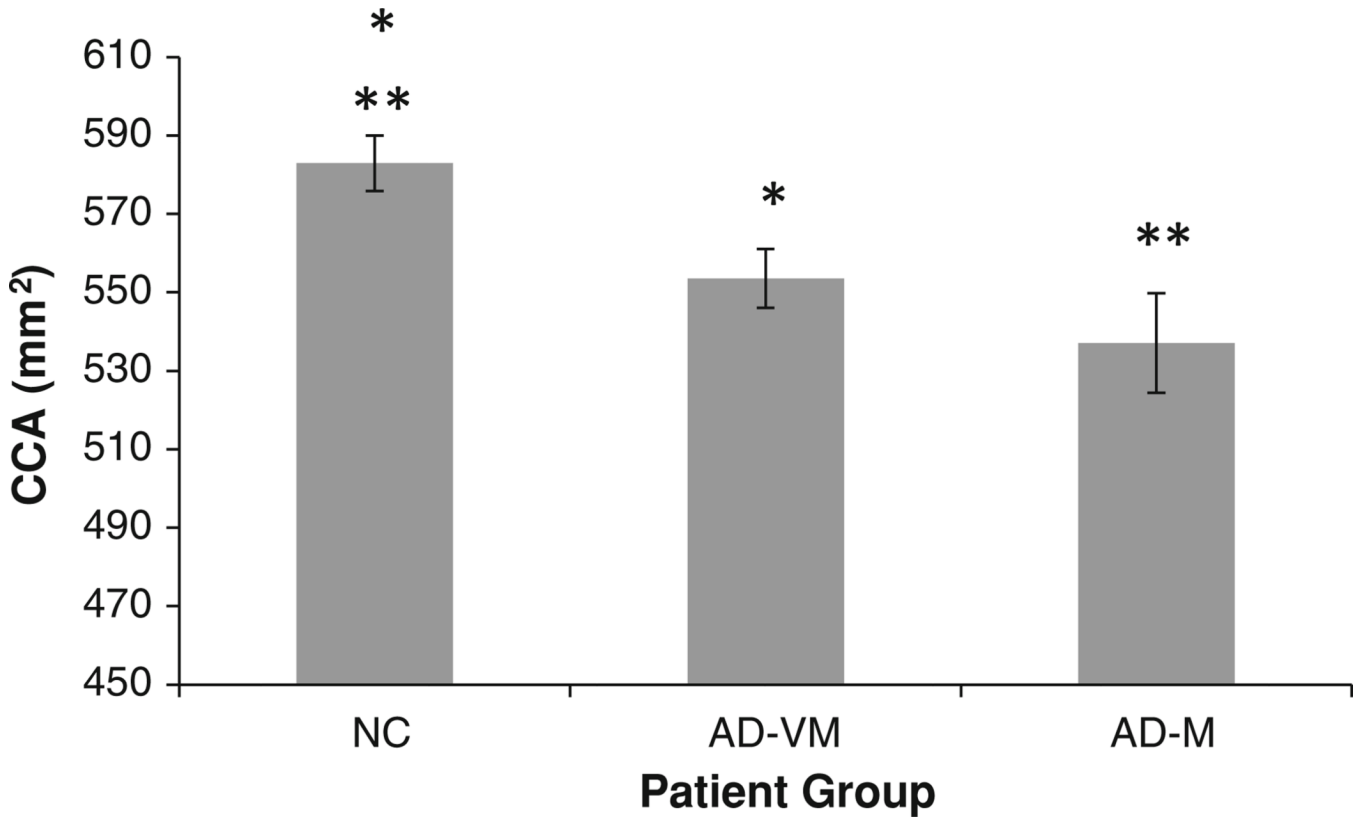

Fig. 4.

Adjusted corpus callosum area (CCA) mean values for the three diagnostic groups. The *error bars* indicate 1 SE. *The mean CCA in AD-VM was statistically smaller than NC (p = 0.005). **The mean in AD-M was statistically smaller than NC (p = 0.002). The AD-VM and AD-M groups were not statistically different (p = 0.266)

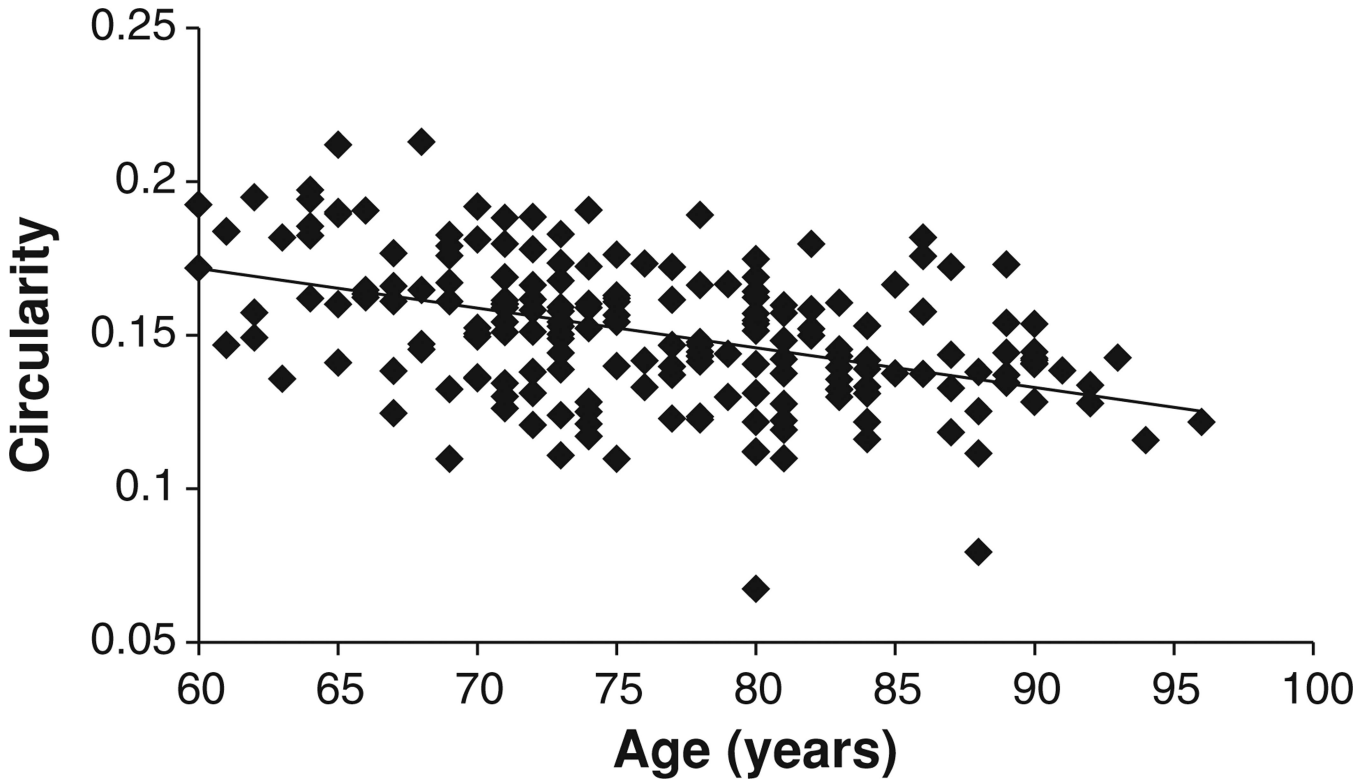

Fig. 5.
Correlation between CIR and age ($\rho = -0.452$; $p < 10^{-10}$)

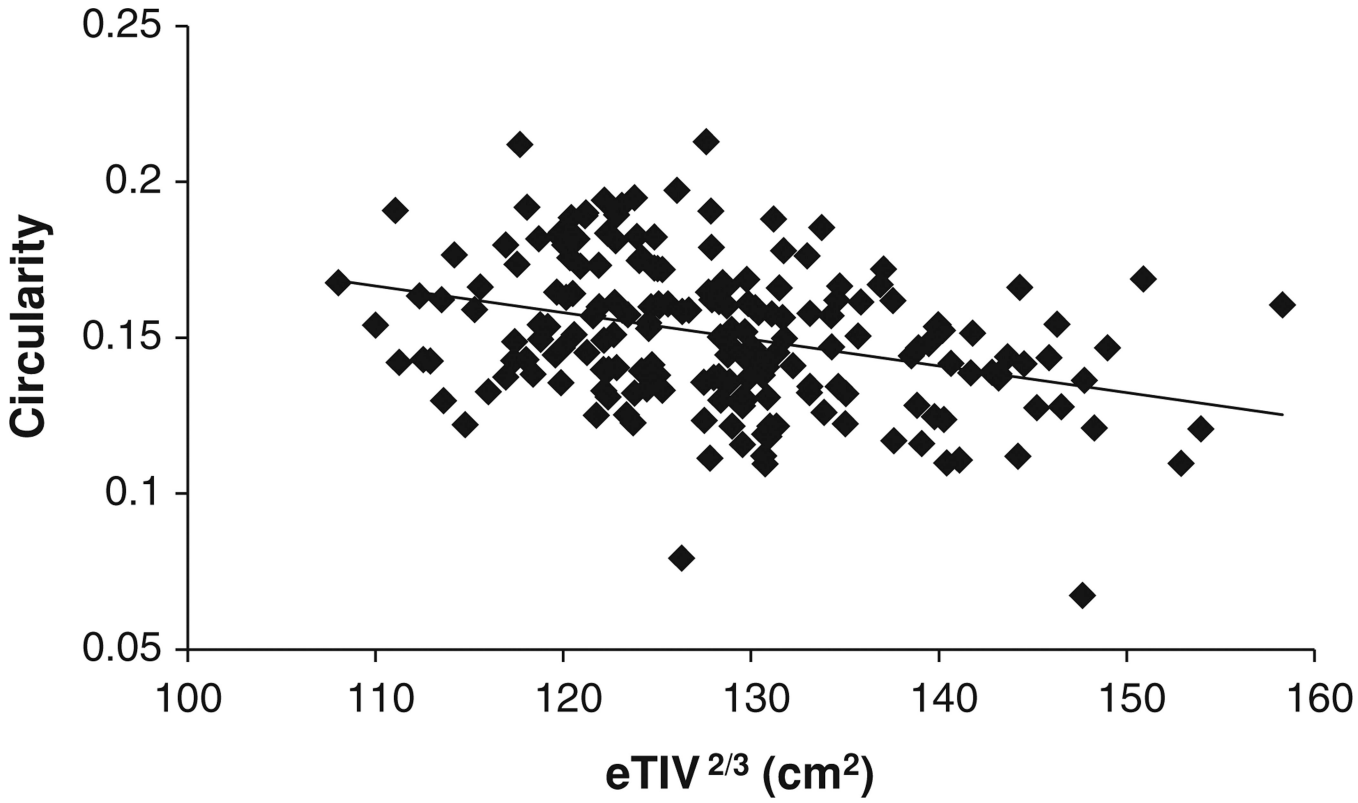

Fig. 6.
Correlation between CIR and intracranial capacity variable $eTIV^{2/3}$ ($\rho = -0.348$; $p < 10^{-6}$)

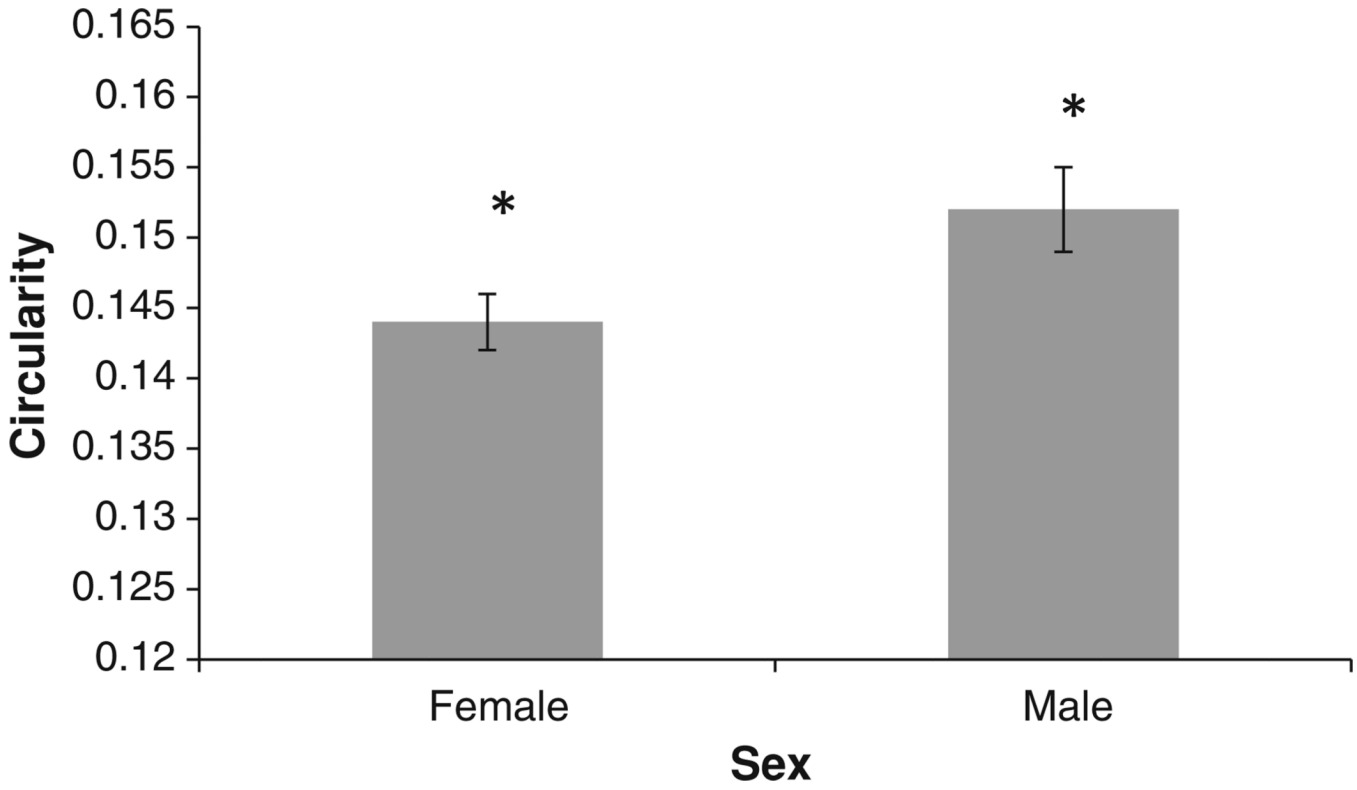

Fig. 7.
Corrected corpus callosum circularity (CIR) mean values for female and male groups. The *error bars* indicate 1 SE. *The mean CIR of the female group was significantly smaller than the male group ($p = 0.015$)

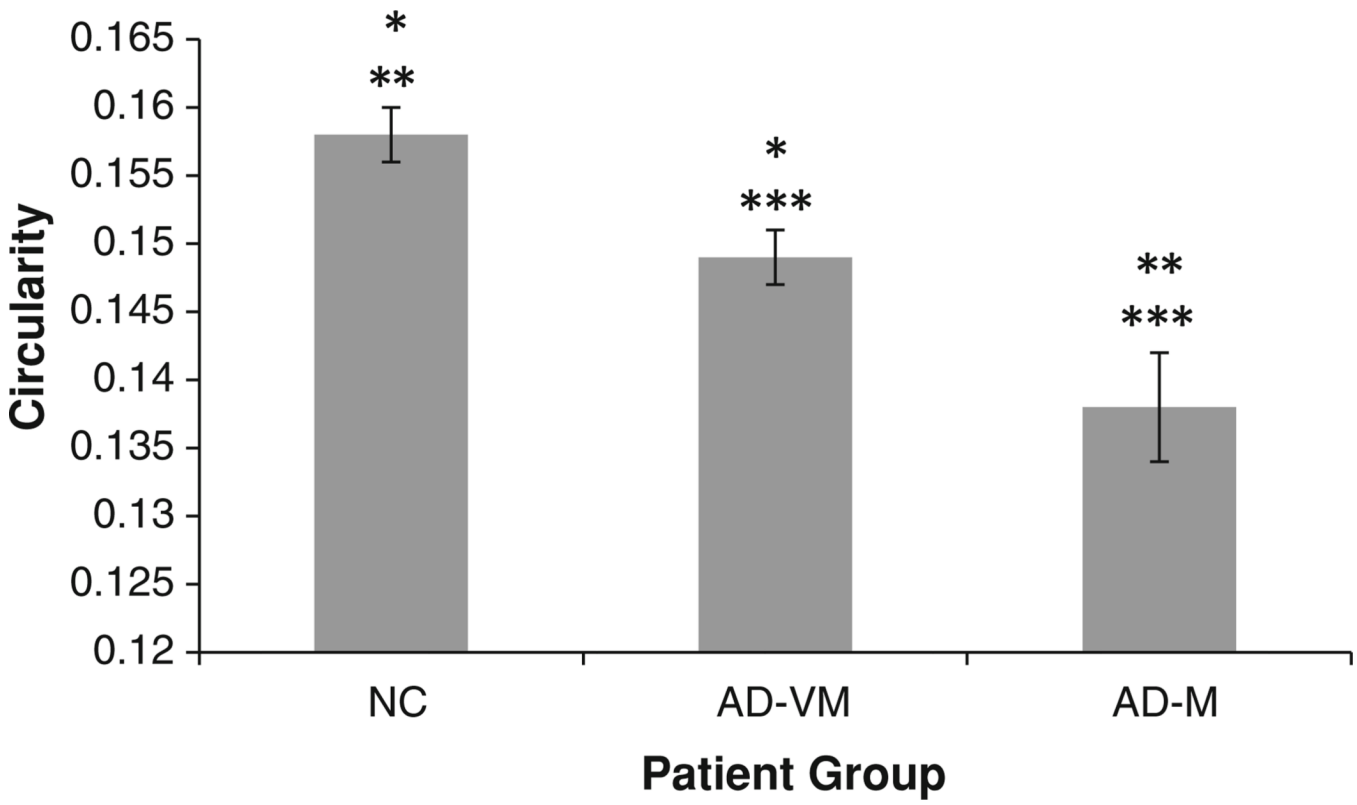

Fig. 8.

Corrected corpus callosum circularity (CIR) mean values for the three diagnostic groups. The *error bars* indicate 1 SE. *The mean CIR in AD-VM was statistically smaller than NC ($p = 0.004$). **The mean in AD-M was statistically smaller than NC ($p < 10^{-5}$). ***The mean AD-M was statistically smaller that AD-VM ($p = 0.006$)

Table 1

Summary statistics

	Normal controls	Very mild AD	Mild AD
CDR	0	0.5	1
Number	98	70	28
Sex (female/male)	72/26	39/31	19/9
Age (years)	75.9 ± 9.0	76.2 ± 7.2	77.8 ± 7.0
MMSE	28.96 ± 1.21	25.64 ± 3.50	21.68 ± 3.75
$eTIV^{2/3}$ (cm^2)	127.3 ± 0.9	130.0 ± 1.3	129.9 ± 1.3
CCA (mm^2)	585.3 ± 7.7	558.5 ± 9.3	543.4 ± 11.6
CIR (×1,000)	157.8 ± 2.3	147.0 ± 2.5	134.5 ± 3.6
*CCA (mm^2)	582.9 ± 7.1	553.5 ± 7.5	537.1 ± 12.7
*CIR (×1,000)	157.8 ± 2.0	149.2 ± 2.1	137.5 ± 3.6

CCA, CIR, and $eTIV^{2/3}$ are given as mean ± SE. Age and minimental state examination (MMSE) scores are given as mean ± SD

*Corrected for age and intracranial capacity evaluated at: age = 76.2, $eTIV^{2/3}$ = 128.6